Analyst

Accepted Manuscript

This article can be cited before page numbers have been issued, to do this please use: Y. Yu, P. Wang, X. Zhu, Q. Peng, Y. Zhou, T. Yin, Y. Liang and X. Yin, *Analyst*, 2017, DOI: 10.1039/C7AN01683B.

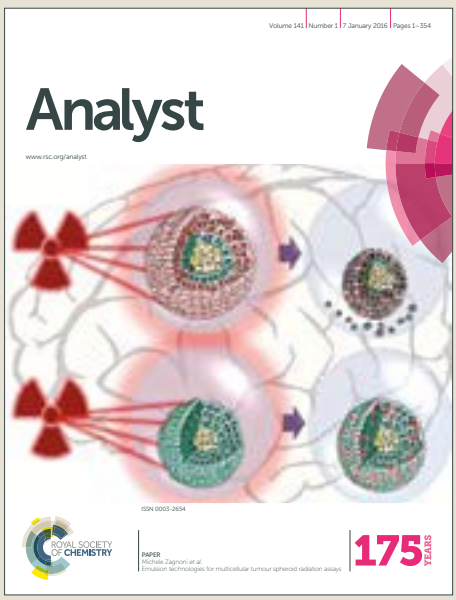

ROYAL SOCIETY OF CHEMISTRY

rsc.li/analyst

View Article Online
DOI: 10.1039/C7AN01683B

Journal Name

ARTICLE

Combined determination of Copper ion and β-Amyloid peptide by a Single ratiometric Electrochemical Biosensor

Received 00th January 20xx,
Accepted 00th January 20xx

DOI: 10.1039/x0xx00000x

www.rsc.org/

Yanyan Yu,*[a,†] Peng Wang,[b,†] Xiaodan Zhu, [b,†] Qiwen Peng, [a] Yi Zhou,[b] Tianxiao Yin, [a] Yixin Liang [c] and Xiaoxing Yin *[a]

Copper ions (Cu^{2+}) play a critical role in biological process and are directly involved in β-amyloid peptide (Aβ) aggregation, which is responsible for the occurrence and development of Alzheimer's disease (AD). Therefore, combined determination of Cu^{2+} and Aβ in one analytical system is of great significance to understand the exact nature of AD event. This work presented a novel ratiometric electrochemical biosensor for the dual determination of Cu^{2+} and $Aβ_{1-42}$. The unique sensor was based on 2, 2'-azinobis-(3-ethylbenzthiazoline-6-sulphonate) (ABTS) and poly (diallyldimethylammonium chloride) (PDDA) - bifunctionalized single-walled carbon nanotubes (ABTS-PDDA/CNTs) composite. The appearance of ABTS not only enhanced the sensitivity, but also acted as an inner reference molecule to improve the detection accuracy. The specific recognition of Cu^{2+} was realized by neurokinin B (NKB) coatings on the ABTS-PDDA/CNTs surface to form a $[Cu^{II}(NKB)_2]$ complex with Cu^{2+}. The ABTS-PDDA/CNTs-NKB modified electrode also displayed an excellent electrochemical response toward $Aβ_{1-42}$ monomer, when a certain amount of $Aβ_{1-42}$ monomer was added into Cu^{2+} - contained PBS buffer, which was due to the release of Cu^{2+} from the $[Cu^{II}(NKB)_2]$ complex through Aβ binding to Cu^{2+}. Meanwhile, our work has displayed that Cu^{2+} bound $Aβ_{1-42}$ was concentration-dependent. Consequently, the presented electrochemical approach was capable of quantifying two important biological species associated with AD by one single biosensor, with the detection limits of 0.04 μM for Cu^{2+} and 0.5 ng/mL for $Aβ_{1-42}$, respectively. Finally, the ratiometric electrode was successfully applied for monitoring Cu^{2+} and $Aβ_{1-42}$ variations in plasma and hippocampus of normal and AD rats.

Introduction

The formation of neutric plaques in the brain has been considered one of the primary hallmarks of Alzheimer's disease (AD).[1] In this process, β-amyloid peptide (Aβ) monomer aggregations in the way of oligomerization and fibrillization are central to the formation of these plaques.[2, 3] More studies have indicated that in vitro and in vivo, Aβ monomer self-assembles into higher order structures (e.g. dimers, trimmers and tetramers) and eventually forms the elongated fibrils that are observed in late-stage AD patients.[4] Both of the soluble oligomers and mature fibrils from Aβ are more neurotoxic compared with monomer and can cause death of brain cells.[5-8] Consequently, development of efficient techniques to observe the level variations of Aβ monomers could provide a clue to unveil the extent of aggregation as well as a definitive molecular basis for understanding the disease mechanism and diagnosing AD. Fluorescence, colorimetry, electrochemistry, surface plasmon resonance (SPR), mass spectrometry (MS) and capillary electrophoresis (CE) have been employed to monitor Aβ species from body fluids and cell media.[9-15]

However, more and more researches have indicated that the hypothesis of self-aggregation of Aβ alone is inadequate to explain the accumulation of Aβ in brain regions. Transition metals (Cu^{2+}, Fe^{3+} and Zn^{2+}) have been directly involved in modulating Aβ aggregations owing to the fact that abnormally high concentrations of metal ions exist within senile plaques.[16-18] This evidence has been further confirmed when Aβ aggregates were treated with metal chelators, which produced soluble Aβ peptides.[19,20] The redox active transition metals generate toxic reactive oxygen species (ROS), which causes oxidative stress and precedes the formation of the amyloid aggregates that are associated with AD.[21-23] Nowadays, preventing Aβ-metal interactions to inhibit oligomer formation has been already proposed as a disease-modifying strategy for AD. Among various metals, the contribution of Cu^{2+} in amyloid deposition has been proposed as a crucial step in the amyloid cascade.[24] Although Cu^{2+} induced Aβ aggregation is still questionable, its complexation with peptide might be responsible for enhancing the formation of the α-helix conformation of the alanine-based peptides.[25,26] Considering the tight correlations between Aβ and Cu^{2+} in the pathological process of AD, a quantitative understanding of the simultaneous level variations of them to uncover the detailed mechanism is essential. However, most of the published work only focused on one specific substance (e.g., Aβ or Cu^{2+}), which is insufficient to explain the exact role of

[a] Jiangsu Key Laboratory of New Drug Research and Clinical Pharmacy, Xuzhou Medical University, 209 Tongshan Road, Xuzhou 221004, Jiangsu, P.R.China
[b] Department of Pharmaceutical Analysis, School of Pharmacy, Xuzhou Medical University, 209 Tongshan Road, Xuzhou 221004, Jiangsu, P.R.China
[c] School of Liberal Arts and Science, Shanghai University of Medicine & Health Sciences, 279 Zhouzhu Highway, Shanghai 201318, P.R.China
† These authors contributed equally to this work.

Electronic Supplementary Information (ESI) available: XPS characterization of the nanocomposite, electrochemical experiments for the electrode, UV-vis spectra, real sample detection. See DOI: 10.1039/x0xx00000x

View Article Online
DOI: 10.1039/C7AN01683B

Aβ-metal interactions played in the AD progress. More importantly, up to now, combined determination of two analytes associated with one disease in a single biological system is still a great challenge due to the unsatisfactory sensitivity.

Electrochemical biosensors have received more and more attentions because of the striking advantages of simplicity, selectivity, low instrumental cost, and capability in real-time, even in vivo detection.[27-30] For its practical applications, signal amplification is crucial for obtaining low detection limit and high sensitivity. Nowadays, the general strategy is nanomaterial involved electrocatalytic amplification.[31-33] The unique chemical and physical properties of the nanoscaled materials, such as metal/semiconductor nanoparticles, can be used to prepare advanced electrocatalytic materials, which thus enable electrochemical monitoring with nanoscale spatial resolution, yielding unique information for better understanding heterogeneous electrode/solution interfaces.[34] Owing to its unique properties, such as high specific surface areas, excellent electrical conductivities and chemical stability,[35] etc., carbon nanotubes (CNTs) have demonstrated a wide availability in many aspects, including supporting noble-metal nanoparticles to prepare functional nanohybrid [36-38] and fabricating biosensors to accelerate electron transfer rate of redox reactions.[39,40] However, insufficient binding site on CNTs for supporting molecules is a well-known drawback, resulting in a poor stability and catalytic activity.[38] Consequently, surface functionalization of CNTs is commonly required by chemical or electrochemical oxidation, wrapping with polymer or grafting of tethers approaches.[41-43]

In this work, we reported a facile but effective strategy for combined determination of Cu^{2+} and Aβ in a single analytical system. To achieve this goal, poly (diallyldimethylammonium chloride) (PDDA) and 2,2'-azinobis-(3-ethylbenzthiazoline-6-sulphonate) (ABTS)-functionalized CNTs were firstly prepared for the loading of Cu^{2+} - specific recognition element, neurokinin B (NKB), and then constructing a ratiometric ABTS-PDDA/CNTs-NKB electrode. The resulting bioelectrocatalytic film was utilized for effective electroreduction of Cu^{2+} with a high sensitivity and accuracy. Then the peak current decreased after a certain amount of $A\beta_{1-42}$ monomer was added into Cu^{2+} - contained PBS solution, which was originated from the stronger coordination between Cu^{2+} and Aβ peptide. It was found that by adjusting the concentration of Cu^{2+} in the detection electrolyte (0.38, 0.95 and 5.7 μM), the ABTS-PDDA/CNTs-NKB electrode was capable of detecting down to 0.001 and up to 3.8 μg/mL $A\beta_{1-42}$. Noticeably, metal ions, amino acids and other endogenous substances in vivo, even Aβ oligomers, could not produce any response changes under the same conditions, indicating a satisfactory selectivity. Compared with the common strategy that utilized two independent electrodes to construct a two-channel system for the dual determination, this method only involved one single electrode, which was much easier to operate and provided a possible route for better understanding the close relationship of two analytes in physiological and pathological events of brain.

Experimental

Materials and Reagents

Pristine single-walled CNTs (ϕ = 10-30 nm) were bought from Chengdu Institute of Organic Chemistry Nanotech Port Co., Ltd. (Chengdu, China). Purified synthetic $A\beta_{1-42}$ was obtained from ChinaPeptides Co,.Ltd. (Shanghai, China). Stimulated aggregation of $A\beta_{1-42}$ samples was achieved by incubation at 37°C in PBS with shaking. NKB, ABTS, PDDA, glutaraldehyde solution (Glu, 25%), glucose (Glu), lactic acid (Lac), uric acid (UA), ascorbic acid (AA), dopamine (DA), all the amino acids and copper sulfate ($CuSO_4$) were all purchased from Sigma-Aldrich (USA) and used without further purification. Phosphate buffer saline (PBS, 0.1 M, pH 7.4) containing 8.6 mM $Na_2HPO_4 \cdot 12H_2O$, 1.88 mM NaH_2PO_4, 50.9 mM NaCl and 2.94 mM KCl was employed as the detection electrolyte. Stock solution of $A\beta_{1-42}$ (1 mg/mL) was prepared by independently dissolving desired amount into 25 mM Tris-HCl buffer solution (pH 7.4) and diluted to approprite concentrations using 10 mM NaOH and freshly-prepared daily before experiments. Water (≥ 18 M) used throughout the whole experiment was purified with Millipore system. All other reagents were of at least analytical grade and commercially available. The plasma and hippocampus homogenate samples from normal and AD rats were kindly provided by L. Zhang in other group.

Apparatus

Scanning electron microscope images (SEM, Hitachi Co. Ltd., Tokyo, Japan) were taken using a field emission gun Hitachi S-4800 scanning electron microscope (operating at 1 kV) for morphological analysis of electrodes. The changes in the diameter of CNTs bundles before and after functionalization were measured by using a FEI Tecnai G2 T12 transmission electron microscope (TEM, USA) operating at 120 kV. The TEM specimens were prepared by dropping the sample solutions onto 50 Å carbon coated copper grids with the excess solution being immediately wicked away. X-ray photoelectron spectroscopy (XPS) investigation was carried out on an ESCALab MKII X-ray photoelectron spectrometer using Mg Kα radiation. Fourier transform infrared spectroscopy (FT-IR) was recorded on a Nicolet model 460 Fourier transform-infrared spectrometer. Raman measurements were carried out on confocal microscope Raman spectrometer system (Renishaw, invia Reflex Raman) with an excitation wavelength of 785 nm.

All the electrochemical experiments were performed on CHI 832D electrochemical workstation (Shanghai Chenhua Instrument, CHI, China). A conventional three-electrode system throughout the experiments composed of a platinum wire as counter electrode, a saturated calomel electrode (SCE) as reference electrode, and a bare or a modified glassy carbon electrode (GC) as working electrode. Unless otherwise indicated, all electrochemical measurements were performed in an oxygen atmosphere.

Preparation of ABTS-PDDA/CNTs hybrid

Before ABTS hybridization, CNTs were firstly functionalized by PDDA according to the previous report.[44] Briefly, 0.5 mg/mL CNTs was dispersed into a 0.5% PDDA aqueous solution containing 0.5 M NaCl by 50 min sonication to give a homogeneous black suspension. Then, the solution was filtered and washed several times with distilled water to remove the free PDDA and dried under vacuum at

View Article Online
DOI: 10.1039/C7AN01683B

70°C for 24 h. After that, 10 mg of the prepared PDDA/CNTs were added into 1 mL of 1.8 mM ABTS aqueous solution. The formed suspension was kept stirring for two days. Then, it was centrifuged. The supernatant was removed and replaced with water. This process was repeated for at least two times and finally, a stable colloidal suspension of ABTS-PDDA/CNTs was obtained.

Electrode modification

The electrode modification was shown in **Scheme 1**. Before fabrication, bare GC was firstly polished with 0.05 μm alumina paste on a micro-cloth and then cleaned using acetone, ethanol and distilled water with ultrasonication for 10 min, respectively and dried at room temperature (25 ± 1°C). 0.2 mg/mL ABTS-PDDA/CNTs or PDDA/CNTs black suspension solutions were obtained by adding 0.2 mg ABTS-PDDA/CNTs or PDDA/CNTs into 1 mL of *N,N*-dimethylformamide (DMF). 5 μL of ABTS-PDDA/CNTs or PDDA/CNTs suspension was dropped onto the cleaned electrode surface, which was denoted as ABTS-PDDA/CNTs-GC or PDDA/CNTs-GC. To realize the specific determination of Cu^{2+}, 5 μL of NKB solution in PBS (0.1M, pH 7.4) (0.5 mg/mL) was introduced onto the ABTS-PDDA/CNTs or PDDA/CNTs layer and allowed to dry at ambient temperature. The obtained electrode was named as ABTS-PDDA/CNTs-NKB-GC or PDDA/CNTs-NKB-GC. Finally, 2 μL of glutaraldehyde (0.1%) was drop-casted to complete the cross-linking of NKB with the ABTS-PDDA/CNTs or PDDA/CNTs hybrid.

Electrochemical determination of Cu^{2+} and $A\beta_{1-42}$ in one analytical system

The electrochemical sensing of Cu^{2+} and $A\beta_{1-42}$ were performed at ambient temperature in a PBS (0.1 M, pH 7.4) buffer solution as displayed in **Scheme 1**, in a typical run, firstly, different concentrations of Cu^{2+} standard solution or real samples from rats were added into 5 mL PBS buffer, followed by gentle stirring for a certain time. The differential pulse voltammetry (DPV) signals were recorded by the potential scan in the range of -0.4 and 0.7 V *vs* SCE. After that, additions of certain amounts of $A\beta_{1-42}$ standard solutions or real samples from rats into Cu^{2+} - contained PBS were followed to observe the signal change at the original potential of -0.12 V belonging to Cu^{2+}. The quantifications of Cu^{2+} and $A\beta_{1-42}$ were respectively estimated by calculating the ratios of the respective current intensity between reduction peaks at -0.12 V for Cu^{2+} and $A\beta_{1-42}$ and 0.58 V for the reference substance ABTS.

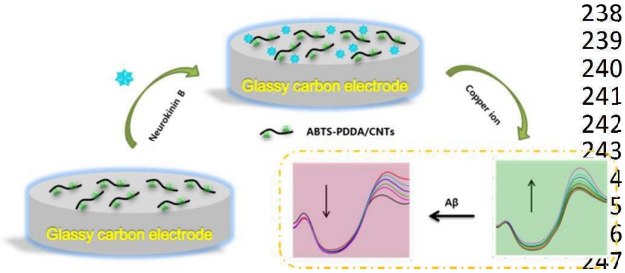

Scheme 1 Combined determination of Cu^{2+} and β-amyloid peptide based on the ratiometric ABTS-PDDA/CNTs-NKB biosensor.

Animal experiments

The induction of AD rats was performed according to our previous work.[14] Briefly, male Wistar rats, weighing 100-120 g at the beginning of experiments, were obtained from Shanghai Yisen Biotechnology Co., Ltd. Rats were housed in plastic cages, with food and water available ad libitum, and kept under standard environmental conditions (12-h light/dark cycle, 22°C). All animal experiments were conducted with approval of the Animal Ethics Committee in Xuzhou Medical University, China. All efforts were made to minimize the number of animals used and their suffering.

D-galactose (D-gal, Aladdin reagent Co., Ltd) and Ibotenic acid (IBO, Enzo Life Science Inc.) were dissolved in sterile saline and ice PBS (pH 7.4) at their final concentrations of 10 g/L and 8 g/L, respectively. Rats were randomly divided into two groups: Normal group and D-gal + IBO group (AD model group) (n = 15 for each group). The latter group was daily administrated D-gal (50 mg/kg in 0.5 mL saline, i.p.) for six weeks, which has been demonstrated to be able to produce aging rats.

After D-gal administration, rats in the AD group were anesthetized with sodium pentobarbital (50 mg/kg, i.p.) and placed on a stereotaxic apparatus (Shenzhen RWD Life Science Co.), with the incisor bar set at 5 mm above the interaural line and appropriately placed holes were drilled through the skull. Stereotaxic coordinates of nucleus basalis magnocellularis (NBM) were set at -1.0 mm posterior and -2.6 mm lateral to bregma and 7.8 mm below from the top of the skull. Bilateral infusions of 1 μL volume of IBO into NBM using a 5 μL Hamilton syringe were lasted over a period of 5 min and the needle was left in place for 5 min after completing the infusion. After the surgery, rats were allowed to recover for 45 days before experiments. Hippocampal homogenates were centrifuged at 4,000 r/min for 15 min and supernatant of the homogenates was used for the following determination.

Results and Discussion

Characterizations of electrodes

CNTs have always been used as carriers to load numerous enzymes or proteins in the preparation of an integrated bio-electrocatalytic system. To promote the electron transfer and stability of pristine CNTs, PDDA and ABTS were successively functionalized with CNTs to produce a more stable colloidal suspension. On one hand, the non-covalent functionalization by PDDA led to a high density and homogeneous distribution of surface functional groups, such as amine group, which was favorable for the self-assembling of negatively-charged ABTS and NKB. On the other hand, the appearance of ABTS not only enhanced the sensitivity, but also acted as an inner reference molecule, thus provided a built-in correction for environmental effects and improved the detection accuracy. The functionalization of CNTs was confirmed by Raman and FT-IR characterizations. As presented in Fig. S1, both CNTs and ABTS-PDDA/CNTs showed similar Raman scattering patterns. The peaks near 1350 and 1580 cm^{-1} could be ascribed to the A_{1g} breathing mode of disorder graphite structure (D band) and the E2g structure mode of graphite (G band).[45] The extent of the modification or defects in CNTs can be evaluated by the intensity ratio of D and G bands (I_D/I_G). This ratio was found to be higher at ABTS-PDDA/CNTs surface (0.28) than that of CNTs (0.08), which was caused by the surface modification process.[38] The FT-IR spectrum of

View Article Online
DOI: 10.1039/C7AN01683B

CNTs showed absorption bands at 1165 and 1705 cm^{-1} corresponding to C-O and C=O stretching vibrations on CNTs (Fig. S2). The band at 1624 cm^{-1} was attributed to the aromatic skeletal C=C stretching vibration of CNTs.[46] The intensity of bands at 1165 and 1705 cm^{-1} decreased on ABTS-PDDA/CNTs, suggesting the interaction between CNTs and PDDA. These above results clearly illustrated that ABTS-PDDA/CNTs have been successfully synthesized.

The surface morphologies of ABTS-PDDA/CNTs and ABTS-PDDA/CNTs-NKB films on ITO were characterized by SEM technique shown in Fig. 1. The functionalized CNTs displayed a homogeneous surface and good dispersion (Fig. 1A), indicating that the modifications of PDDA and ABTS preserved the intrinsic properties of CNTs. After NKB was attached to the ABTS-PDDA/CNTs part and cross-linked with glutaraldehyde, surface topography significantly changed with increased degree of cross-linking on the whole film due to the massive loading of proteins throughout the three-dimensional structure of CNTs (Fig. 1B). Comparison of TEM images of ABTS-PDDA/CNTs and ABTS-PDDA/CNTs-NKB composites at the same magnification showed that the surface of ABTS-PDDA/CNTs became rougher and bundles of CNTs changed into thicker following NKB modification. Shown in Such results confirmed the successful fabrication of the ABTS-PDDA/CNTs-NKB-GC. The changes in chemical compositions with the step-by-step modification were also tracked by XPS analysis (See Fig. S3 in ESI).

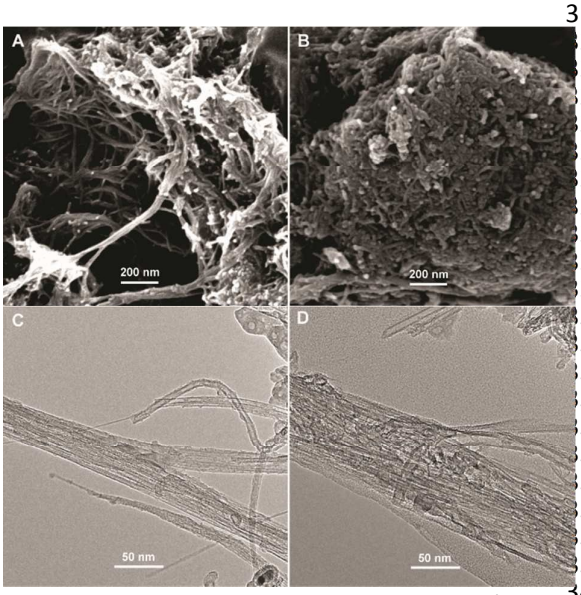

Fig. 1 SEM (A, B) and TEM (C, D) images of ABTS-PDDA/CNTs (A, C) and ABTS-PDDA/CNTs-NKB (B, D) composites.

Cyclic voltammetry (CV) was also employed to investigate the electrochemistry of the stepwise fabricated electrode interfaces in $Fe(CN)_6^{3-}/Fe(CN)_6^{4-}$ redox couple in pH 7.4 PBS buffer. As seen from Fig. S4, the pristine bare GC exhibited a well-defined couple of redox peaks in the range of -0.4 ~ 0.7 V. The attachment of conductive PDDA/CNTs or ABTS-PDDA/CNTs hybrid appreciably enhanced the redox currents by improving the electronic coupling to the underlying electrode, which was beneficial for the following analyte detection with increased sensitivity. After further immobilization of NKB onto the prepared ABTS-PDDA/CNTs interface, as expected, the peak current significantly decreased due to the impeding essence of native proteins for electron transfer on electrodes. Such a result attested that PDDA/CNTs or ABTS-PDDA/CNTs and NKB have been fabricated onto electrode step by step, which coincided with TEM, SEM and XPS results.

Electrochemical performance of ABTS-PDDA/CNTs-NKB electrode toward Cu^{2+} determination

Our previous work has employed NKB as the unique biomolecular recognition for Cu^{2+} to form a $[Cu^{II}(NKB)_2]$ complex, which assured the selectivity of Cu^{2+} determination against a series of potential interferences in vivo.[42] In the present contribution, after the ABTS-PDDA/CNTs-NKB electrode was successfully fabricated, the Cu^{2+} - sensitive behavior was investigated in 100 mM PBS buffer (pH 7.4) by DPV. The electrochemical responses of Cu^{2+} with the same concentration (8.0 μM) were compared among four kind electrodes, e.g., bare GC (I), PDDA/CNTs-GC (II), ABTS-PDDA/CNTs-GC (III) and ABTS-PDDA/CNTs-NKB-GC (IV). As illustrated in Fig. 2, only charge current was observed on bare GC in 8.0 μM Cu^{2+} - contained PBS buffer solution (curve I), while an obvious reduction peak located at around -0.1 V *vs* SCE appeared at PDDA/CNTs-GC, which can be ascribed to the electrochemical reduction of PDDA/CNTs (curve II). Afterwards, a new peak at 0.58 V belonging to the reduced state of ABTS ($ABTS^{2-}$) on ABTS-PDDA/CNTs film arose in the 8.0 μM Cu^{2+} - contained PBS buffer (curve III). After a certain amount of NKB solution was casted onto the ABTS-PDDA/CNT-GC and determined in the 8.0 μM Cu^{2+} solution, as expected, the electrochemical signal at -0.12 V obviously increased, whereas the current at 0.58 V remained unchanged (curve IV), indicating that Cu^{2+} was recognized by NKB and electron transfer between electrode and Cu^{2+} ion took place. Consequently, the quantification of Cu^{2+} in this ratiometric assay can be realized on the basis of the current ratios (I_P / $I_{P(R)}$) between the two peaks at -0.12 and 0.58 V, in which the current at -0.12 V for Cu^{2+} was denoted as I_P, and $I_{P(R)}$ represented the currents of ABTS at 0.58 V.

Different concentrations of Cu^{2+} standard solutions were added into PBS buffer and the corresponding DPV responses obtained on ABTS-PDDA/CNTs-NKB-GC were recorded. As displayed in Fig. 3, the peak current at -0.12 V increased gradually with the addition of Cu^{2+}, while the peak current at 0.58 V kept constant. The calculated I_P / $I_{p(R)}$ ratios showed a good linear range toward Cu^{2+} within a wide concentration range of 0.1 to 10 μM. In consideration of the wide span of Cu^{2+} levels between normal and AD rats, it would be more ideal for practical applications to have a broader range of dynamic responses. The linear dependencies of Cu^{2+} concentrations yielded the regression equation of I_P / $I_{p(R)}$ = 0.03 $C_{(\mu M)}$ + 1.63, with a correlation coefficient R of 0.9913. The detection limit of such a detection strategy was 0.04 μM, estimated from 3σ of the baseline signals. This value was much lower than our previously published work that utilized functionalized polymerized ionic liquid as the substrate for the loading and permeation of NKB.[47] Moreover, it was also equal to or better than that of other reported Cu^{2+} detection assays,[48-52] which indicated that the established electrochemical strategy held great potential for Cu^{2+} determination in a biological matrix.

View Article Online
DOI: 10.1039/C7AN01683B

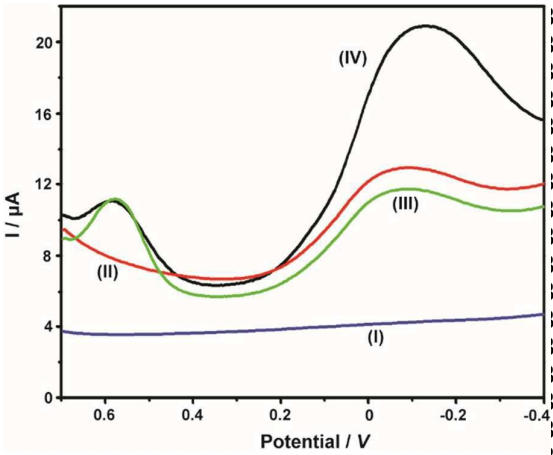

Fig. 2 DPV curves obtained on bare GC (I), PDDA/CNTs-GC (II), ABTS-PDDA/CNTs-GC (III) and ABTS-PDDA/CNTs-NKB-GC (IV) in 100 mM PBS buffer solution containing 8.0 μM Cu^{2+}.

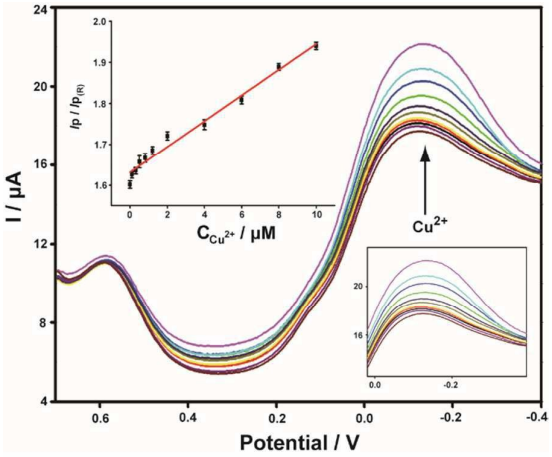

Fig. 3 DPV curves of the ABTS-PDDA/CNTs-NKB-GC toward successive additions of Cu^{2+} at the concentrations of 0、0.1、0.3、0.5、0.8、1.2、2.0、4.0、6.0、8.0、10.0 μM. Inset was the corresponding linear plot of the $I_P/I_{p(R)}$ ratios versus the absolute concentrations of Cu^{2+}.

Ratiometric determination of $A\beta_{1-42}$ by ABTS-PDDA/CNTs-NKB-GC

Aβ has always been considered as the direct pathogenic factor for AD in the way of oligomerization and fibrillization to form neutric plaques. Several research groups have reported the binding of Cu^{2+} to Aβ peptides.[53,54] On the basis of the above-displayed Cu^{2+} determination, it was therefore expected that Cu^{2+} acted as the complexing agent for Aβ, after which, the current responses of Cu^{2+} on the ABTS-PDDA/CNTs-NKB-GC would basically decrease in the presence of Aβ due to the release of Cu^{2+} from the $[Cu^{II}(NKB)_2]$ complex, hence developing a novel methodology for Aβ monitoring. Shown in Fig. 4A was the DPV responses obtained at ABTS-PDDA/CNTs-NKB electrode in 6.0 μM Cu^{2+} solution before (curve a) and after additions of 1.8 and 3.8 μg/mL $A\beta_{1-42}$ (curves b, c). Upon the first addition of $A\beta_{1-42}$, the reduction current at -0.12 V increased whereas the signal at 0.58 V decreased. This phenomenon was normally caused by the perturbation of the detection electrolyte by the variation in pH as Aβ standard solution was prepared in NaOH. However, at the second testing, the reduction peak located at -0.12 V decreased, while that observed at 0.58 V kept constant. The decline in the current was attributed to the release of Cu^{2+} from the $[Cu^{II}(NKB)_2]$ complex when bound to Aβ, probably due to the reason that Aβ has stronger coordination capability to Cu^{2+} than NKB, and thus Cu^{2+} was replaced from the $[Cu^{II}(NKB)_2]$ complex with the addition of Aβ. In order to verify the signal change was reliably induced by Aβ, not other factors, two control experiments were carried out hereafter. Firstly, in the absence of Cu^{2+}, the continuous additions of 1.8 and 3.8 μg/mL $A\beta_{1-42}$ into the blank PBS didn't cause any visible change in the reduction currents at both -0.12 V and 0.58 V (Fig. 4B). Meanwhile, as suggested from Fig. 4C, although the initial addition of NaOH solution, solvent for solubilizing Aβ, into 6.0 μM Cu^{2+} - contained PBS buffer induced the same result as that of $A\beta_{1-42}$, no further change was observed when NaOH was introduced into electrolyte for the second time. These results clearly demonstrated that this single ratiometric sensor provided a sensitive and accurate platform for determination of Cu^{2+} and $A\beta_{1-42}$ in one electrochemical system.

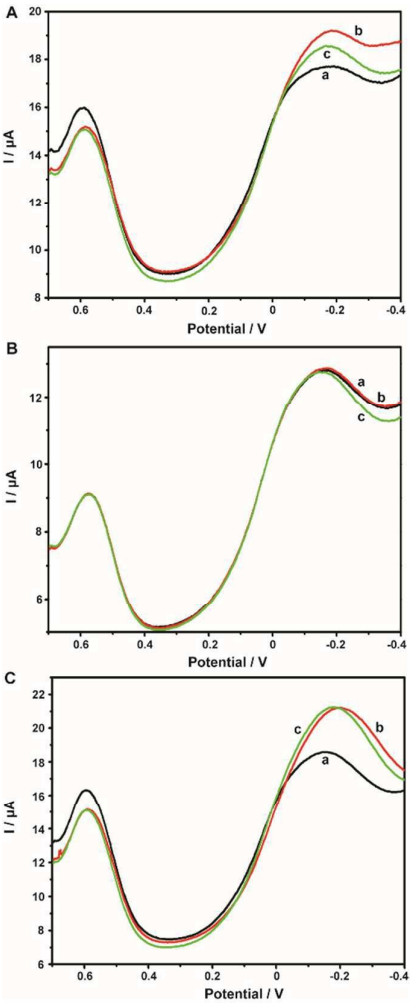

Fig. 4 DPV curves obtained on ABTS-PDDA/CNTs-NKB-GC toward 1.8 (red curve, b) and 3.8 μg/mL $A\beta_{1-42}$ (green curve, c) in the presence (A) and absence (B) of 6.0 μM Cu^{2+} PBS buffer. (C) was the DPV responses of 10 μL NaOH additions (b and c) into 6.0 μM Cu^{2+} PBS buffer.

View Article Online
DOI: 10.1039/C7AN01683B

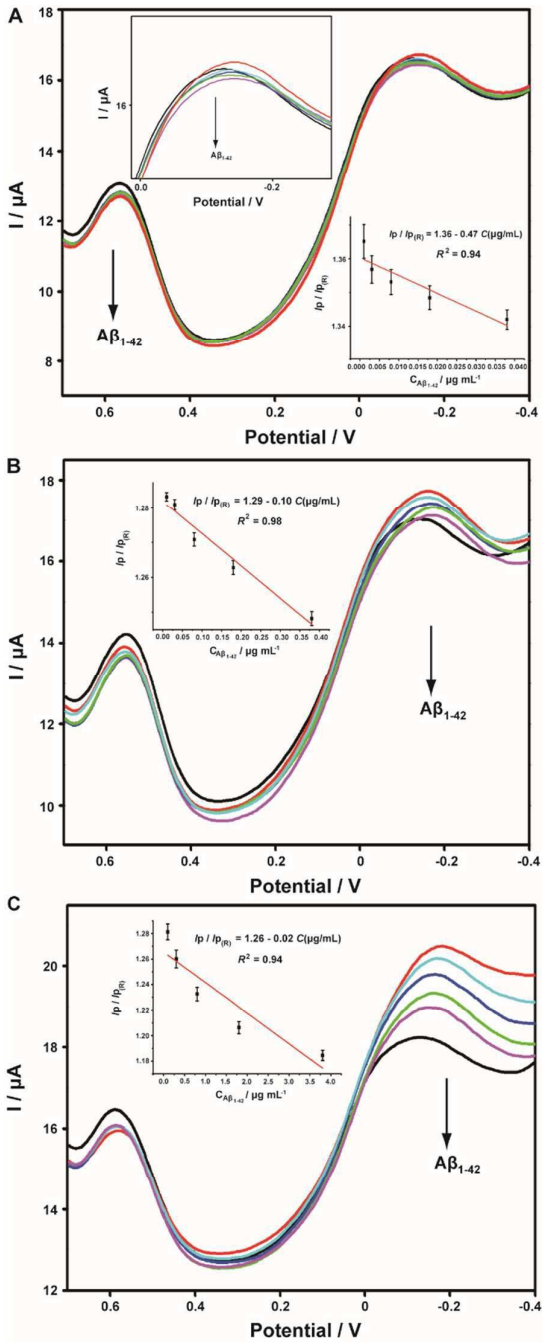

Fig. 5 DPV curves of the ABTS-PDDA/CNTs-NKB-GC towards successive additions of $A\beta_{1-42}$ in 0.38 (A), 0.95 (B) and 5.70 μM (C) Cu^{2+} - contained PBS buffer. The inspected concentrations of $A\beta_{1-42}$ was 0.001, 0.003, 0.008, 0.018, 0.038 μg/mL for 0.38 μM Cu^{2+}; 0.01, 0.03, 0.08, 0.18, 0.38 μg/mL for 0.95 μM Cu^{2+}; 0.1, 0.3, 0.8, 1.8, 3.8 μg/mL for 5.70 μM Cu^{2+}. Inset was the corresponding linear plots of the $I_p/I_{p(R)}$ ratios *versus* the absolute concentrations of $A\beta_{1-42}$.

It has been widely discussed that Cu^{2+} was capable of inhibiting or accelerating the aggregation of Aβ peptide by binding to Aβ and forming the Cu^{2+} - Aβ complex.[23] Therefore, it was quite interesting that whether this binding was concentration-dependent or not. Herein, we examined the interaction between Cu^{2+} and Aβ with three concentrations of Cu^{2+} by electrochemical technique. As shown in Fig. 5C, when performed in 5.70 μM Cu^{2+} solution, the peak current obtained at -0.12 V gradually and linearly decreased on additions of increasing concentrations of $A\beta_{1-42}$ (from 0.1 to 3.8 μg/mL). More interestingly, we found that the linear current changes of $A\beta_{1-42}$ on the ABTS-PDDA/CNTs-NKB-GC could only be acquired in a fixed concentration of Cu^{2+}. For example, in Fig. 5B, when a lower concentration of Cu^{2+} (0.95 μM) was contained in PBS, the lowest detectable concentration of $A\beta_{1-42}$ was down to 0.01 μg/mL, one order of magnitude lower than that in 5.70 μM Cu^{2+} solution. Likewise, when the concentration of Cu^{2+} continued dropping down to 0.38 μM, the linear range of $A\beta_{1-42}$ started at a much lower concentration (1 ng/mL) in comparison with that in 0.95 and 5.70 μM Cu^{2+} (Fig. 5A). We also tested the response of $A\beta_{1-42}$ in Cu^{2+} solution with a much lower concentration than 0.38 μM. Unfortunately, no similar tendency was observed as those depicted above (data not shown). The corresponding linear regression equations, linear correlation coefficients of $A\beta_{1-42}$ on ABTS-PDDA/CNTs-NKB biosensor at different concentrations of Cu^{2+} were displayed in the inset of Fig. 5.

It has reported that Cu bound Aβ could function as peroxidase and possessed peroxidase activity.[55] Therefore, to verify the above DPV results, we measured the peroxidase activity of Cu^{2+} - Aβ complex with three concentrations for the catalytic oxidation of ABTS in the presence of H_2O_2 by UV-vis. As displayed in Fig. S5, in the range of 600 - 800 nm, two strong absorption peaks located at around 620 and 700 nm were both observed, which were ascribed to the catalytic oxidation of ABTS by the formed Cu-Aβ complex in the presence of H_2O_2. Additionally, by lowering the incubated concentration of Cu^{2+} and $A\beta_{1-42}$ in sequence, the peak intensity at 620 and 700 nm gradually decreased, especially the peak at 700 nm, indicating that the concentrations of Cu^{2+} and Aβ played a key role in the catalytic capability of the Cu^{2+} - Aβ complex for the oxidation of ABTS by H_2O_2, which were consistent with the electrochemical results.

Selectivity, reproducibility and stability investigations

The selectivity of the developed electrochemical system for Cu^{2+} and Aβ determination was evaluated in two ways: one was by individually monitoring and comparing the electrochemical signals of Cu^{2+} and interferences in PBS, and the other was by adding interferences into Cu^{2+}-contained PBS solution and comparing the signals with that of single Cu^{2+}. Metal ions (Ca^{2+}, Fe^{3+}, Mg^{2+}, Na^{+}, Cd^{2+}, Co^{2+}, Mn^{2+}, Ni^{2+}, Pb^{2+}, Zn^{2+}, Cu^{+}), amino acids (Cys, Phe, Glu, Met, Lys, Gly, Arg, Ser, Leu, Val, Thr, His) and other common endogenous substances, including ascorbic acid (AA), dopamine (DA), uric acid (UA), lactic acid (Lac) and glucose (Glu) were chosen as the potential interferences. As shown in Fig. S4, compared with Cu^{2+}, additions of the tested interferences into PBS buffer didn't arouse significant changes in the current intensity. Likewise, the I_p / $I_{p(R)}$ values were almost unperturbed in the simultaneous presence of these species and Cu^{2+} relative to that of single Cu^{2+}. More importantly, we also examined the potential interferences from aggregated Aβ. The results in Fig. S6C clearly illustrated that the developed electrochemical method was only suitable for the monitoring of monomeric forms of Aβ, rather than oligomeric or other forms. All these evidences indicated the high selectivity of the fabricated ABTS-PDDA/CNTs-NKB-GC for Cu^{2+} and Aβ biosensing against metal ions, amino acids and endogenous species coexisting in the biological system.

View Article Online
DOI: 10.1039/C7AN01683B

In addition, the relative standard deviations (RSDs) were evaluated to be 4.9% and 7.1% at three different electrodes in parallel for Cu^{2+} and $A\beta_{1-42}$, respectively, indicating the acceptable reproducibility for the dual determination of two analytes. The biosensor also showed reasonable stabilities for the analytes, in which 91.5% and 87.4% of the current responses for Cu^{2+} and $A\beta_{1-42}$ were retained after the modified electrode was stored in 4°C for one week.

Estimation of Cu^{2+} and $A\beta_{1-42}$ variations in the plasma and hippocampus of normal and AD rats

Finally, we applied the developed ABTS-PDDA/CNTs-NKB-GC into the estimation of Cu^{2+} and $A\beta_{1-42}$ variations in the plasma and hippocampus of normal and AD rats. Fig. 6 presented the DPV curves obtained on the ABTS-PDDA/CNTs-NKB-GC for Cu^{2+} in the plasma from normal and AD rat brain. As can be seen, the electrochemical responses of Cu^{2+} showed significant differences between normal and AD groups. A clear rise in the concentration of Cu^{2+} was witnessed in AD rat plasma compared with that in normal rat, which were in good agreement with previously reported results, as well as our findings.[47,56] Based on our postcalibration, the concentration of Cu^{2+} was calculated to be 1.11 ± 0.19 μM in normal rat plasma and this value increased to 9.20 ± 1.15 μM in AD plasma (n = 3). For $A\beta_{1-42}$ determination, as for the coexistence of many different isoforms of Aβ in the biological system including $A\beta_{1-42}$, the way of real sample detection was different from Cu^{2+}, in which various amounts of $A\beta_{1-42}$ were firstly spiked with hippocampus homogenate and then added into Cu^{2+} - contained PBS buffer. As listed in Table S1, the recoveries of these measurements were in the range of 91.7% ~ 110% under the optimal conditions, indicating that this method was reliable and practical.

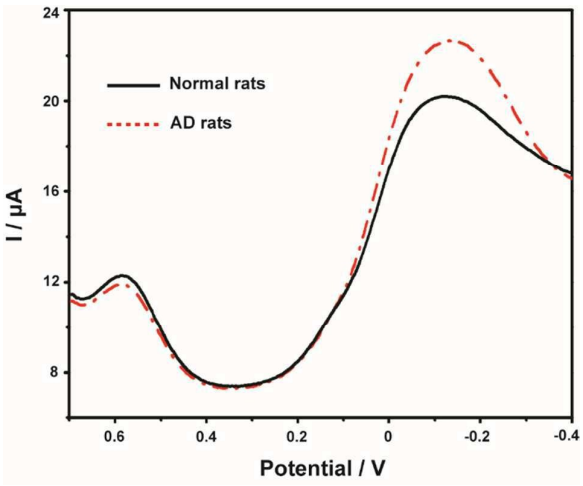

Fig. 6 DPV responses of the ABTS-PDDA/CNTs-NKB-GC on Cu^{2+} in the plasma of normal and AD rats.

Conclusions

In summary, with the demand for revealing the roles of Aβ peptide and metal ions for the treatment of AD, we presented herein a ratiometric electrochemical detection system to sensitively probe Cu^{2+} and Aβ co-variations, which were both associated with the development of AD. Due to the stronger complexation of Cu^{2+} with Aβ, Cu^{2+} was released from the as-formed $[Cu^{II}(NKB)_2]$ complex once Aβ was added. Therefore, besides Cu^{2+}, Aβ could also be easily monitored by the same ABTS-PDDA/CNTs-NKB biosensor immediately after Cu^{2+} determination. The theoretically simple, low technical and instrumental demands as well as the high sensitivity and selectivity made this methodology suitable and reliable enough for the real sample detection. Our results showed that the present approach provided us a crucial route for simultaneously monitoring two important biological species, which were closely linked with each other, in one single analytical system.

Conflicts of interest

There are no conflicts to declare.

Acknowledgements

We appreciate the financial supports from the National Natural Science Foundation of China (no. 21675137 and 21205102), Natural Science Foundation of Jiangsu Province (no. BK20161170), China Postdoctoral Science Special Foundation (no. 2016T90504) and China Postdoctoral Science Foundation funded projects (no. 2015M580471), Jiangsu Planned Project for Postdoctoral Research Funds (no. 1501087B), the Program for Distinguished Talents of Six Domains in Jiangsu Province (no. 2016-SWXY-060), Jiangsu "333" project of cultivation of high-level talents, Qing Lan Project of Jiangsu Province and the Priority Academic Program Development of Jiangsu Higher Education Institutions (PAPD).

Notes and references

(1) I. Choi, L. P. Lee, *Acs Nano.*, 2013, **7**, 6268-6277.
(2) M. K.-D., J. Meier, S. H. Choi, E. M. Norstrom, S. S. Sisodia, R. F. Ismagilov, *Angew. Chem. Int. Edit.*, 2009, **48**, 1487-1489.
(3) S. Chimon, Y. Ishii, *J. Am. Chem. Soc.*, 2005, **127**, 13472-13473.
(4) A. A. Reinke, P. M. U. Ung, J. J. Quintero, H. A. Carlson, J. E. Gestwicki, *J. Am. Chem. Soc.*, 2010, **132**, 17655-17657.
(5) S. I. Yoo, M. Yang, J. R. Brender, V. Subramanian, K. Sun, N. E. Joo, S. H. Jeong, A. Ramamoorthy, N. A. Kotov, *Angew. Chem. Int. Edit.*, 2011, **50**, 5110-5115.
(6) G. Bitan, M. D. Kirkitadze, A. Lomakin, S. S. Vollers, G. B. Benedek, D. B. Teplow, *P. Natl. Acad. Sci. USA.*, 2003, **100**, 330-335.
(7) C. Haass, D. J. Selkoe, *Nat. Rev. Mol. Cel.l Bio.*, 2007, **8**, 101-112.
(8) A. T. Petkova, R. D. Leapman, Z. H. Guo, W. M. Yau, M. P. Mattson, R. Tycko, *Science.*, 2005, **307**, 262-265.
(9) N. Xia, L. Liu, M. G. Harrington, J. Wang, F. Zhou, *Anal. Chem.*, 2010, **82**, 10151-10157.
(10) T. E. Golde, C. B. Eckman, S. G. Younkin, *Biochim. Biophys. Acta.*, 2000, **1502**, 172-187.
(11) L. A. Munishkina, A. L. Fink, *Biochim. Biophys. Acta.*, 2007, **1768**, 1862-1885.

View Article Online
DOI: 10.1039/C7AN01683B

(12) R. Picou, J. P. Moses, A. D. Wellman, I. Kheterpal, S. S. Gilman, *Analyst*., 2010, **135**, 1631-1635.
(13) Y. Y. Yu, X. Y. Sun, D. Q. Tang, C. L. Li, L. Zhang, D. X. Nie, X. Yin, G. Y. Shi, *Biosens. Bioelectron*., 2015, **68**, 115-121.
(14) Y. Y. Yu, L. Zhang, C. L. Li, X. Y. Sun, D. Q. Tang, G. Y. Shi, *Angew. Chem. Int. Edit. Engl.*, 2014, **53**, 12832-12835.
(15) Y. Y. Yu, L. Zhang, X. Y. Sun, C. L. Li, Y. Qiu, H. P. Sun, D. Q. Tang, Y. W. Liu, X. X. Yin, *Chem Commun (Camb).*, 2015, **51**, 8880-8883.
(16) Y. L. Zhou, J. Wang, L. T. Liu, R. R. Wang, X. H. Lai, M. T. Xu, *Acs. Chem. Neurosci*., 2013, **4**, 535-539.
(17) J. H. Viles, *Coordin. Chem. Rev.*, 2012, **256**, 2271-2284.
(18) K. J. Barnham, A. I. Bush, *Curr. Opin. Chem. Biol*., 2008, **12**, 222-228.
(19) R. A. Cherny, C. S. Atwood, M. E. Xilinas, D. N. Gray, W. D. Jones, C. A. McLean, K. J. Barnham, I. Volitakis, F. W. Fraser, Y. S. Kim, X. D. Huang, L. E. Goldstein, R. D. Moir, J. T. Lim, K. Beyreuther, H. Zheng, R. E. Tanzi, C. L. Masters, A. I. Bush, *Neuron*., 2001, **30,** 665-676.
(20) R. A. Cherny, J. T. Legg, C. A. McLean, D. P. Fairlie, X. D. Huang, C. S. Atwood, K. Beyreuther, R. E. Tanzi, C. L. Masters, A. I. Bush, *J. Biol. Chem*., 1999, **274**, 23223-23228.
(21) L. C., S. Guilloreau, A. Sournia-Saquet, H. Mazarguil, P. Faller, *Chembiochem*., 2007, **8**, 1317-1325.
(22) C. C. Curtain, F. Ali, I. Volitakis, R. A. Cherny, R. S. Norton, K. Beyreuther, C. J. Barrow, C. L. Masters, A. I. Bush, K. J. Barnham, *J. Biol. Chem*., 2001, **276**, 20466-20473.
(23) D. Pramanik, C. Ghosh, S. G. Dey, *J. Am. Chem. Soc.*, 2011, **133**, 15545-15552.
(24) A. Tiiman, P. Palumaa, V. Tougu, *Neurochem. Int*., 2013, **62**, 367-378.
(25) J. Zou, N. Sugimoto, *Protein Peptide Lett.*, 1999, **6**, 373-378.
(26) J. Zou, N. Sugimoto, *J. Chem. Soc. Perk .T 2.*, 2000, **10**, 2135-2140.
(27) Y. P. Luo, Y. Tian, Q. Rui, *Chem. Commun*., 2009, **21**, 3014-3016.
(28) M. Xu, R. h. Wang, Y. b. Li, *Analyst*., 2002, **9**, 990-991.
(29) X. M. Zhuang, H. H. Wang, T. He, L. X. Chen, *Microchim Acta*, 2016, **183**, 3177-3182.
(30) X. M. Zhuang, D. L. Wang, Y. Q. Lin, L. F. Yang, P. Yu, W. Jiang, L. Q. Mao, *Anal. Chem.*, 2012, **84**, 1900-1906.
(31) Q. Wang, Y. Song, Y. Q. Chai, G. Q. Pan, T. Li, Y. L. Yuan, R. Yuan, *Biosens. Bioelectron.*, 2014, **60**, 118-123.
(32) P. Jing, W. J. Xu, H. Y. Yi, Y. M. Wu, L. J Bai, R. Yuan, *Analyst*., 2014, **139**, 1756-1761.
(33) N. Zhou, J. H. Li, H. Chen, C. Y. Liao, Z. P. Chen, L. X. Chen, *Analyst*., 2013,**138**, 1091-1097.
(34) S. M. Oja, M. Wood, B. Zhang, *Anal. Chem.*, 2013, **85**, 473-486.
(35) L. T. Qu, L. M. Dai, *J. Am. Chem. Soc*., 2005, **127**, 10806-10807.
(36) Y. T. Kim, K. Ohshima, K. Higashimine, T. Uruga, M. Takata, H. Suematsu, T. Mitani, *Angew. Chem. Int. Edit.*, 2006, **45**, 407-411.
(37) L. Cao, F. Scheiba, C. Roth, F. Schweiger, C. Cremers, U. Stimming, H. Fuess, L. Q. Chen, W. T. Zhu, X. P. Qiu, *Angew. Chem. Int. Edit*., 2006, **45**, 5315-5319.
(38) B. H. Wu, D. Hu, Y. J. Kuang, B. Liu, X. H. Zhang, J. H. Chen, *Angew. Chem. Int. Edit*., 2009, **48**, 4751-4754.
(39) J. Wang, M. Musameh, *Analyst*., 2004, **129**, 1-2.
(40) K. Karnicka, K. Miecznikowski, B. Kowalewska, M. Skunik, M. Opallo, J. Rogalski, W. Schuhmann, P. J. Kulesza, *Anal. Chem*., 2008, **80**, 7643-7648.
(41) D. Wang, Z. C. Li, L. W. Chen, *J. Am. Chem. Soc*., 2006, **128**, 15078-15079.
(42) L. Tao, G. J. Chen, G. Mantovani, S. York, D. M. Haddleton, *Chem. Commun. (Camb)*., 2006, **47**, 4949-4951.
(43) S. Y. Wang, X. Wang, S. P. Jiang, *Langmuir*., 2008, **24**, 10505-10512.
(44) S. Wang, S. P. Jiang, X. Wang, *Nanotechnology*., 2008, **19**, 265601.
(45) I. V. Anoshkin, I. I. Nefedova, D. V. Lioubtchenko, I. S. Nefedov, A. V. Räisänen, *Carbon.*, 2017, **116**, 547-552.
(46) H. Thakur, N. Kaur, D. Sareen, N. Prabhakar, *Talanta.*, 2017, **171**, 115-123.
(47) Y. Y. Yu, C. Yu, T. X. Yin, S. S. Ou, X. Y. Sun, X. R. Wen, L. Zhang, D. Q. Tang, X. X. Yin, *Biosens. Bioelectron.*, 2017, **87**, 278-284.
(48) Z. j. Lin, F. Q. Luo, T. Q. Dong, L. Y. Zheng, Y. X. Wang, Y. W. Chi, G. N. Chen, *Analyst*., 2012, **137**, 2394-2399.
(49) H. Xu, J. Yan, X. She, L. Xu, J. Xia, Y. Xu, Y. Song, L. Huang, H. Li, *Nanoscale*., 2014, **6**, 1406-1415.
(50) L. E. Guo, J. F. Zhang, X. Y. Liu, L. M. Zhang, H. L. Zhang, J. H. Chen, X. G. Xie, Y. Zhou, K. Luo, J. Yoon, *Anal. Chem*., 2015, **87**, 1196-1201.
(51) L. Zhang, Y. Han, F. Zhao, G. Shi, Y. Tian, *Anal. Chem*., 2015, **87,** 2931-2936.
(52) A. Zhu, Q. Qu, X. Shao, B. Kong, Y. Tian, *Angew. Chem. Int. Ed. Engl.*, 2012, **51**, 7185-7189.
(53) C. S. Atwood, R. C. Scarpa, X. D. Huang, R. D. Moir, W. D. Jones, D. P. Fairlie, R. E. Tanzi, A. I. Bush, *J. Neurochem*., 2000, **75**, 1219-1233.
(54) C. D. Syme, R. C. Nadal, S. E. J. Rigby, J. H. Viles, *J. Biol. Chem*., 2004, **279**, 18169-18177.
(55) D. Pramanik, S. G. Dey, *J. Am. Chem. Soc*., 2011, **133**, 81-87.
(56) Y. P. Luo, L. M. Zhang, W. Liu, Y. Y. Yu, Y. Tian, *Angew. Chem. Int. Ed.*, 2015, **54,** 14053-14056.